“西光所建所六十周年暨《光子学报》创刊五十周年”专辑
引用格式：LI Dongyu, YU Tingting, ZHU Jingtan, et al. *In vivo* Skull Optical Clearing Technique and its Applications (Invited)[J]. Acta Photonica Sinica, 2022, 51(8):0851514
李东宇,俞婷婷,朱京谭,等. 活体颅骨光透明方法及应用(特邀)[J].光子学报,2022,51(8):0851514

活体颅骨光透明方法及应用(特邀)

李东宇[1,2,3],俞婷婷[1,2,3],朱京谭[1,2,3],朱芬[1,2,3]
(1 华中科技大学 武汉光电国家研究中心,Britton Chance 生物医学光子学研究中心&生物医学光子学教育部重点实验室,武汉 430074)
(2 华中科技大学 高端生物医学成像设施,武汉 430074)
(3 湖北光谷实验室,武汉 430074)

摘　要：颅骨的高散射极大地限制了光学技术在活体脑成像中的应用。开颅窗和磨薄颅骨窗等基于手术的“颅窗”让皮层神经-血管观测成为可能,但各有局限性。近年来发展的活体颅骨光透明技术,以一种更方便、更无创方式建立光透明颅窗。本文主要介绍活体颅骨光透明的发展及应用:1)颅骨光透明方法;2)基于光透明颅窗的细胞及血管成像;3)透过光透明颅窗,实现皮层光操控,包括结合光动力效应打开血脑屏障或实施靶向栓塞、基于激光损伤的靶向出血性脑卒中建立、以及在光遗传学方面的应用等。最后,对活体颅骨光透明技术未来的发展和应用做出展望。

关键词：活体颅骨光透明;光学成像;光操控;神经血管成像;光动力效应
中图分类号：Q336　　**文献标识码**：A　　**doi**：10.3788/gzxb20225108.0851514

0　引言

在体观测大脑的结构和活动,对了解大脑以及脑疾病相关的神经血管功能障碍具有重要意义[1-3]。现代光学成像技术侵入性低、分辨率高,因而能够用于活体观测生物结构和功能[4-10],在脑科学领域发挥着重要作用[11-13]。例如,激光散斑对比成像可以实现对皮层血流变化的动态监测[14-15],高光谱成像[16-17]可以用于监测血管中的血氧饱和度[18-19],光学相干断层扫描可以在微米级别的分辨率下对组织进行三维成像[20-21]。非线性光学显微镜(双光子荧光成像、三光子荧光成像、二倍频成像、三倍频成像等)可以观测大脑皮层的深层神经细胞和血管结构功能[22-26],并被用于相关疾病的研究[27-28]。

但是,在活体状态下,大脑上面有颅骨覆盖,而颅骨对光的强散射严重限制了光的穿透深度,进而影响了皮层成像的质量和深度[29-30]。为了克服颅骨的散射,以往的研究往往需要在成像前建立各类手术颅窗,主要包括开颅玻璃窗、磨薄颅骨窗以及它们的变体[31-32]。开颅玻璃窗可以保持一个月以上,因此适用于长期重复成像[33]。但是,开颅手术容易导致炎症反应,且往往会持续约2周[32,34],因此开颅玻璃窗不适合对急性模型的观测。磨薄颅骨窗的建立通过将部分颅骨磨薄至约25 μm左右,在这种情况下,颅骨不会过多地限制光的穿透,因而可以实现对皮层的活体高分辨观测。但磨薄颅骨窗不适用于大视场观测皮层,因为将大面积的颅骨均匀地磨薄至25 μm的难度非常大[35-37]。另外,颅骨被磨薄后会重新生长,并且新生的颅骨质地会发生变化、且易碎,成像质量会随着反复磨薄越来越差、且难以实现多次的重复打磨[32]。所以,磨薄颅骨窗不适用于长期跟踪观测。

近年兴起的组织光透明技术可以降低生物组织的散射,增强光在组织中的穿透能力,已被广泛应用于离体大组织甚至全器官三维高分辨成像[38-44]。不仅如此,组织光透明技术在活体水平也得到了很好的应用。

基金项目：国家自然科学基金(Nos. 61860206009, 81870934, 82001877),武汉光电国家研究中心创新专项目,光谷实验室创新专项(No. OVL2021BG011)
第一作者：李东宇(1992—),男,博士后,主要研究方向为深组织成像及应用。Email: li_dongyu@mail.hust.edu.cn
通讯作者：朱芬(1966—),女,教授,博士,主要研究方向为组织光透明成像。Email: dawnzh@mail.hust.edu.cn
收稿日期：2022-06-06;**录用日期**：2022-07-25

研究人员发展的活体颅骨光透明技术，以及基于此建立的光透明颅窗，可以在不进行开颅手术的情况下，结合多种现代光学成像手段，实现大脑皮层的神经血管结构和功能的观测。研究人员针对不同的应用场景，开发了不同的光透明颅窗，可以分别满足高分辨、大视场、长时程观测等要求。相比于开颅玻璃窗，光透明颅窗可以避免手术带来的炎症反应，从而适用于急性观测；相比于磨薄颅骨窗，光透明颅窗可以通过反复建立而观测数月，从而实现长期跟踪监测。本文将从活体颅骨光透明技术与应用的角度进行介绍。

1 活体颅骨光透明技术

活体组织光透明技术最早用于皮肤的透明化成像，能够提高小鼠、大鼠等实验动物皮肤对光的穿透能力[45]，甚至可以提升对人体皮肤的成像深度[46-47]。经典的活体皮肤光透明试剂包括甘油、丙二醇、聚乙二醇-400等[47]，它们的作用是使组织脱水并解离胶原蛋白，配合物理或者化学促渗方法，可以大大提升皮肤的透明度。但是，颅骨（硬组织）和皮肤（软组织）的结构完全不同，它在失水的状态下反而会更加浑浊，因而颅骨透明化的思路必须与皮肤不同。科研人员经过不断探索，终于在2012年用多种试剂的混合溶液首次实现了活体小鼠的颅骨透明化并用于光学成像[48]。而后，研究人员进一步从中筛选有效试剂并优化配比，以及加入新的试剂，不断完善方法，开发了一系列光透明颅窗。

颅骨的主要成分包括羟基磷灰石（钙质）、胶原蛋白（16%）、脂质（54%）和水（14%）[49]。因此，活体颅骨光透明的基本原理就是（部分）去除颅骨中的钙质、脂质和蛋白质，并用折射率匹配液进一步提高透明效果（如图1）。

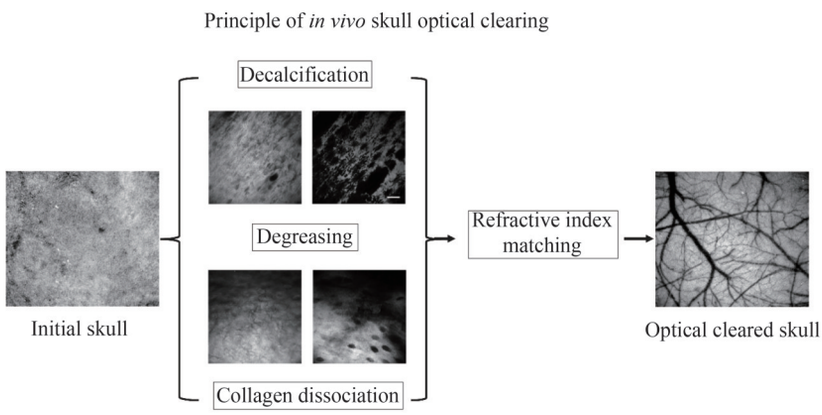

图1 活体颅骨光透明的基本原理[50-51]

Fig.1 Basic principle of *in vivo* skull optical clearing[50-51]

1.1 SOCS：实现活体颅骨光透明

为了去除颅骨中的散射子，WANG Jing等[48]发明了一种颅骨光透明液（Skull Optical Clearing Solution，SOCS），它是一种包含乙二胺四乙酸（Ethylene Diamine Tetraacetic Acid，EDTA），二甲亚砜、山梨醇、月桂醇、乙醇、葡萄糖的弱碱性溶液。在实验过程中，首先将小鼠的头皮剪开，暴露颅骨，然后将颅骨用SOCS孵育25 min即可让混浊的颅骨变得透明，皮层微血管也逐渐从不可见变得清晰，能够分辨的最小血管直径为（14.4±0.8）μm，而在开颅状态下可分辨的最小血管直径为（12.8±0.9）μm，证明颅骨透明化的成像效果接近于开颅状态。

SOCS可以提高激光散斑成像的质量，实现皮层血流分布可视化[48]，YANG Xiaoquan等[52]在体研究了SOCS处理前后皮层血管光声成像的差异，发现透明后相同血管的光声信号显著增强，原本无法观测的深皮层血管也可以清楚地观察到。定量分析结果表明，颅骨光透明处理后，光声信号增加到原始的2.59倍，且不会改变皮层血管的直径。SOCS首次为皮层血管成像提供了一个无需手术的颅窗，证明了活体颅骨光透明的可行性。但其安全性、有效性及可重复性有待进一步评估。

1.2 SOCW：实现穿颅神经树突棘成像

2018年，ZHAO Yanjie等[53]提出了一种优化的颅骨光透明窗（Skull Optical Clearing Window，SOCW），结合双光子荧光显微镜可以获得达到突触级别的成像分辨率。颅骨中的无机基质和有机基质的主要成分

分别是羟基磷灰石钙和胶原蛋白，随着小鼠年龄的增长，无机基质和有机基质的比例也会发生变化。因此，对于幼年小鼠（出生20天之内）和非幼年小鼠（出生大于20天），采用不同的光透明流程。

SOCW的建立步骤分为两步：对于出生15～20天的小鼠，用10%的胶原酶溶液孵育5～10 min；对于出生21～30天的小鼠，将胶原酶溶液置换为10%的EDTA二钠溶液，同样孵育5～10 min；对于出生超过30天的小鼠，颅骨生长得更厚，因此需要先将颅骨磨薄至约100 μm，然后用10%的EDTA二钠溶液孵育5～10 min。进一步，将80%的甘油滴加在颅骨上，进行折射率匹配，即完成了光透明颅窗的建立。SOCW建立的颅窗可以通过用磷酸缓冲液擦洗颅骨来“关闭”，即使得颅骨恢复到浑浊状态。但是，如果需要在第二天进行重复开窗观测，光透明处理的时间需要比前一天略长一些。

利用双光子荧光显微镜，可以透过SOCW实现对皮层20～80 μm深处的神经元树突棘的观测，说明其分辨率可以达到亚微米尺度，这是活体颅骨光透明技术的一个突破；与此同时，该方法在安全性方面得到了有效验证。但是，该方法用于4周龄以上的小鼠时需要对颅骨进行打磨，不仅增加了实验难度，还会遇到与磨薄颅骨窗同样的问题，即难以实现大视场的观测以及长期重复观测。

1.3 USOCA：可开合的大视场颅窗

2018年，ZHANG Chao等[54]发展了一种基于尿素的光透明方法（Urea-based Skull Optical Clearing Agent，USOCA），成功解决SOCW未能解决的两大难题，即视场较小和无法实现长期跟踪。

USOCA包含两种混和试剂，其一是75%乙醇溶解的饱和尿素溶液，乙醇溶液与尿素的体积-质量比约为10∶3 mL/g。其二是高浓度的十二烷基苯磺酸钠（Sodium Dodecyl Benzene Sulfonate，SDBS）溶液，它是由0.7 mol/L的氢氧化钠溶液与十二烷基苯磺酸配置而成的，前者与后者的体积-质量比约为24∶5 mL/g，且pH值保持在7.2～8的范围内。乙醇分子上的羟基可以促使胶原解离，尿素不仅因其有水合作用而被广泛用于组织透明化，还可以起到促渗的作用；十二烷基苯磺酸钠是一种离子型去垢剂，有去脂作用，可以使得颅骨成分更加均一。

剪开小鼠头皮、暴露颅骨后，用第一种试剂滴加在颅骨，其间用镊子夹住小棉球不断在颅骨上按摩，进行物理促渗，颅骨会慢慢变透明。10 min后，擦除第一种试剂，将第二种试剂滴加在颅骨上，并孵育5 min，在这段时间内，颅骨会很快变得更为透明。由于完全不需要对颅骨进行磨薄处理，可以根据实验需要调整光透明颅窗的尺寸，实验人员利用USOCA对缺血性脑卒中及再灌注过程进行了双侧大脑皮层的血流成像。待成像完成后，用磷酸盐缓冲液（Phosphate Buffer Solution，PBS）将光透明试剂清洗干净，颅骨即可恢复至原有状态，即“关闭”光透明颅窗。若需要进行重复成像，只需再进行透明操作即可再次“打开”光透明颅窗。

值得一提的是，USOCA可以适用于2～8月龄的小鼠，这一特性与大视场和可长期重复“开合”的特性，极大地拓展了活体颅骨光透明技术的应用范围。但是，USOCA结合双光子荧光显微术，也仅能获得皮层300 μm的成像深度，这远远不到小鼠皮层的厚度（>1 mm）。因此光透明颅窗的透明度还有待进一步提升，来满足深皮层成像的需求。

1.4 SOCW结合USOCA：进一步提高透明度

为了进一步提高光透明颅窗的透明度，CHEN Yage等[55]将SOCW和USOCA两种颅骨光透明方法进行结合，并从理论和实验两个方面验证了这种结合的可行性。在研究中，他们利用非标记的高光谱受激拉曼散射（Stimulated Raman Scattering，SRS）显微术对两种颅骨光透明方法的分子机制进行了阐释。SRS可以将光透明剂对颅骨不同成分的影响进行可视化。

SOCW的主要成分是胶原酶和EDTA。研究发现，10%的胶原酶孵育5～10 min后，颅骨表面的胶原纤维能得到有效解聚。然而，胶原酶不能降解羟基磷灰石和羟基磷灰石内部的胶原。相反，EDTA孵育5～10 min后，骨陷窝周围形成大量空腔，颅骨内羟基磷灰石的厚度明显降低。这意味着EDTA不仅能分解羟基磷灰石，还能使蛋白质均质化。USOCA的主要有效成分是尿素的75%乙醇溶液（S1）和十二烷基苯磺酸钠溶液（S2）。研究表明，USOCA孵育15 min后，颅骨表面和深层区域的蛋白均被解聚并重新均匀分布。结果还表明，与胶原酶相比，USOCA具有更强的溶解蛋白质的能力。

由于SOCW和USOCA的透明机理有所不同，CHEN Yage等结合两种方法，并开展了活体实验。科研人员依次用USOCA（25 min）、10%的EDTA（25 min）对颅骨进行孵育，去除后滴加80%的甘油并进行成

像，可以得到非常显著的透明效果。结合三光子荧光显微镜，可以对皮层850 μm深的血管进行成像观测。

将SOCW和USOCA进行结合，进一步拓展了光透明颅窗下的成像深度。但是，结合两种方法，使得光透明颅窗的建立时间接近一个小时，降低了便捷性。另一方面，同时去除了颅骨中的胶原蛋白和羟基磷灰石，可能使得颅骨的刚性结构、以及它对大脑的保护作用受到影响，不利于长期跟踪观测。

1.5 VNSOCA：可见-近红外兼容的光透明颅窗

颅骨光透明技术主要着眼于减低颅骨的散射，这对于利用可见光和近红外Ⅰ区（700～900 nm）波段的成像非常重要。但是，在近红外Ⅱ区（900/1 000～1 700 nm），生物组织的散射减少[56-60]，吸收就是另一个需要考虑的重要因素。

LI Dongyu等[51]测量了USOCA方法所用的两种混和试剂的透过率，发现在近红外Ⅱ区、尤其在1 300 nm以上的波段有着非常大的吸收，这对于近红外Ⅱ区成像显然非常不利。研究发现，该吸收主要是光透明试剂中的重要成分——水（H_2O）带来的。为了克服这一问题，研究人员将水替换成在可见光到近红外Ⅱ区均有较高透过率的重水（D_2O），并将以此配置的颅骨光透明试剂命名为适用于可见-近红外Ⅱ区的颅骨光透明试剂（Visible-Near infrared Ⅱ-compatible Skull Optical Clearing Agent，VNSOCA）。

研究人员首先用体外成像实验比较了USOCA和VNSOCA对近红外二区激发的非线性光学成像的适用性。研究人员将一种三倍频探针的溶液放置在毛细玻璃管中，将其放置在1 560 nm飞秒激光激发的三倍频显微镜下，分别将USOCA和VNSOCA作为成像介质进行成像。结果表明，由于USOCA对激发光有较大的吸收，限制了整套成像方案的效率，因而探测到的三倍频信号非常有限。相对的，VNSOCA作为成像介质时，测得的信号强度提升了3倍以上。进而，研究人员进行了活体实验。结果表明，即使基于利用近红外二区（1 560 nm）激发的三倍频成像技术，也只能在浑浊颅骨下获取皮层200 μm深的毛细血管结构，而VNSOCA建立的光透明颅窗，可以将穿颅血管成像深度提升3倍以上。VNSCOA的发明，为颅骨光透明颅技术在近红外Ⅱ区成像领域的应用提供了方法，拓展了光透明颅窗适用的波段范围。几种颅骨光透明技术的比较见表1。

表1 几种颅骨光透明技术的比较

Table 1 Comparisons of skull optical clearing techniques

	Composition proportion	Operation procedure	Operation time	Range of application	Safety assessment
SOCS[48]	EDTA, dimethyl sulfoxide, sorbitol, laurinol, alcohol, glucose and weak alkaline substances	Application of the optical clearing agent on the skull	25 min	Imaging of cortical blood vessels	No assessment
SOCW[53]	Solution 1: 10% collagenase Solution 2: 10% EDTA disodium Solution 3: 80% glycerol	For mice aged P15-P20: the intact skull was topically treated with solution 1 for 5～10 min; Then, solution 3 was dropped on the skull. For mice aged P21-P30: the intact skull was topically treated with solution 2 for 5～10 min; Then, solution 3 was dropped on the skull. For mice aged more than P30: the skull was thinned down to about 100 μm and treated with solution 2 for 5～10 min. Then, solution 3 was dropped onto the skull	5～10 min	Imaging of dendritic spines of neurons at a depth of 0～80 μm Repeated optical clearing for 2～3 times Targeted laser ablation of neurons	Immune response of microglia or astrocytes in the cortex was not activated

续表

	Composition proportion	Operation procedure	Operation time	Range of application	Safety assessment
USOCA[54,61-65]	Solution 1: saturated urea solution dissolved in 75% ethanol Solution 2: SDBS prepared by mixing 0.7 M NaOH with dodecyl benzene sulfonic acid	Solution 1 was applied to the intact skull for 10 min. Then, solution 2 was applied for 5 min	15 min	Imaging of nerves and blood vessels at a depth of 0-300 μm Repeated daily optical clearing imaging for a week Repeated monthly optical clearing imaging for 5 months. Realization of blood-brain barrier opening combined with photodynamic effect or establishment of targeted photothrombosis	Immune response of microglia or astrocytes in the cortex was not activated. No effect on the structure of the liver and kidneys
SOCW+USOCA	Solution 1: saturated urea solution dissolved in 75% ethanol Solution 2: SDBS prepared by mixing 0.7 M NaOH with dodecyl benzene sulfonic acid Solution 3: 10% EDTA disodium Solution 4: 80% glycerol	The intact skull was treated with solution 1 for 20 min, solution 2 for 5 min, solution 3 for 25 min and solution 4 for 5 min in sequence	55 min	Imaging of blood vessels in the cortex at a depth of 900 μm combined with three-photon imaging	No assessment
VNSOCA[51]	Solution 1: saturated urea solution dissolved in 75% ethanol and deuteroxide Solution 2: SDBS prepared by mixing 0.7 M NaOH and deuteroxide with dodecyl benzene sulfonic acid	The intact skull was topically treated with solution 1 for 10 min and solution 2 for 5 min	15 min	Compatible with visible-NIR-Ⅱ band Imaging of cortex at a depth of 650 μm combined with third harmonic generation excited by femtosecond laser in the NIR-Ⅱ band Establishment of targeted hemorrhagic stroke model induced by NIR-Ⅱ laser	No assessment

2 活体颅骨光透明用于神经/血管成像

活体颅骨光透明技术与多种光学成像方法技术的结合,已被证明可广泛用于小鼠脑皮层神经细胞(神经元、胶质细胞)和血管的观测。比如,利用激光散斑衬比成像技术和高光谱成像技术,可以对皮层表面血

管的血流和血氧分布进行无标记成像；利用双光子荧光成像、三倍频成像等非线性光学成像技术，可以对皮层深层神经血管结构实施三维观测。

2.1 突触可塑性观测

神经元树突棘的生长和消融与记忆和认知功能有着紧密的联系，其异常往往与许多脑神经疾病相关[66-67]，因而观测其变化具有重要的生物学意义[68-70]。但是，树突棘的尺寸在亚微米级，这就对成像方法提出了很高的要求。一般来说，在体观测神经元树突棘需要使用双光子荧光显微镜，同时配合开颅玻璃窗或磨薄颅骨窗。光透明颅窗技术为该应用提供了一种新型的低侵入式的观测思路。

ZHAO Yanjie等[53]率先验证了光透明颅窗用于观测神经元突触可塑性的可行性。利用SOCW，研究人员对神经元自发表达黄色荧光蛋白（Yellow Fluorescent Protein，YFP）的小鼠进行了活体成像。结果表明，SOCW的建立使得图像质量得到显著改善，足以对树突棘进行清晰地成像。进一步地，对幼鼠（P19）的神经元树突棘进行了为期1小时的持续观测，观察到树突棘的出现和消失、以及形状的变化。并且，相较于树突棘，神经元的丝状伪足具有更高的运动性，它甚至可以转化为树突棘，说明丝状伪足在发育过程中可能是树突棘的前体。这些结果表明，小鼠神经元突触的可塑性在第三周是非常强的（如图2）。

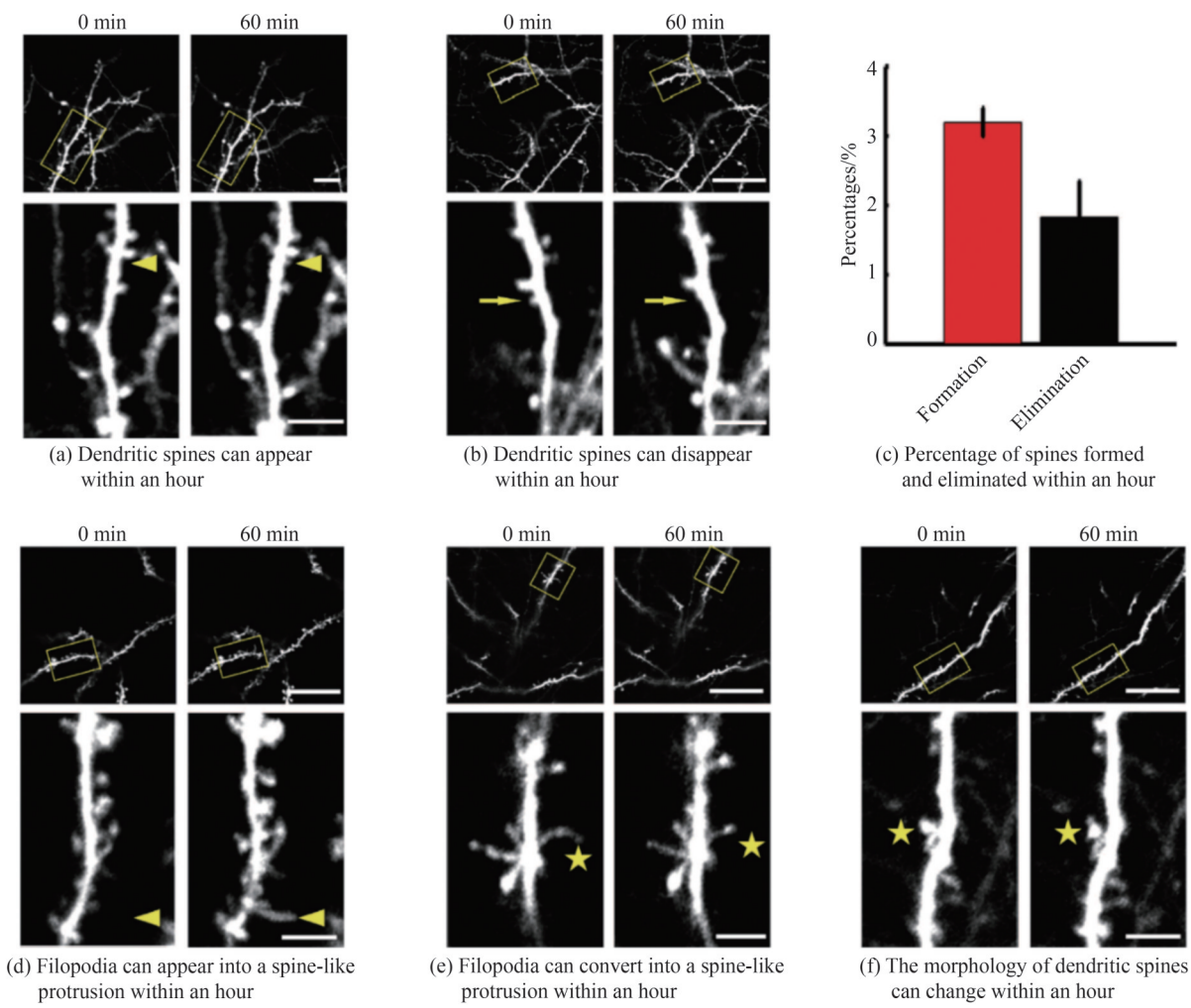

图2 透过SOCW对出生19天的未成年小鼠的突触可塑性的动态观测[53]

Fig.2 Dynamical monitoring of the plasticity of dendritic protrusions in infantile mice (P19) through the SOCW [53]

2.2 皮层血流血氧跟踪监测

血流和血氧变化是反应血管功能的重要指标，监测皮层血流、血氧信息对于研究多种脑疾病有着重要的意义[71-73]。激光散斑衬比成像是一种非标记的、高时空分辨的血流分布成像技术[74-76]；高光谱成像技术是一种非标记的血氧分布成像技术[76-78]。颅骨光透明技术的出现使其得以在完整颅骨下获取皮层血流血氧

信息。

ZHANG Chao等[54]发展的USOCA技术极大地拓展了光透明颅窗在皮层跟踪监测方面的应用。利用搭建的激光散斑衬比成像/高光谱成像双模态系统，结合USOCA，科研人员对大脑中动脉阻塞（Middle Cerebral Artery Occlusion，MCAO）后的双侧皮层血流血氧分布进行了30 min的持续观测。结果表明，随着时间的推移，手术侧血流和血氧值都急剧下降。MCAO术后10 min，手术侧动脉血流的下降值约为初始值的60%，并在术后30 min完全停止流动。，术侧静脉血流在术后10 min时下降约40%，30 min时，下降约60%。血氧饱和度的变化与血流的变化规律基本一致。在MCAO对侧，血流显著增加，动脉血流增加到初始值的近3倍，静脉增加约50%。然而，研究人员发现手术对侧的动静脉血氧饱和度只是略有增加。

不仅如此，利用USOCA，可以持续一周地每天对小鼠进行颅骨透明化操作并获取血流血氧信息。不仅如此，研究人员对2月龄的小鼠进行了每月一次、为期5个月的持续成像，并成功观察到皮层血管网的动态变化，即部分血管的消失和新生（图3）。

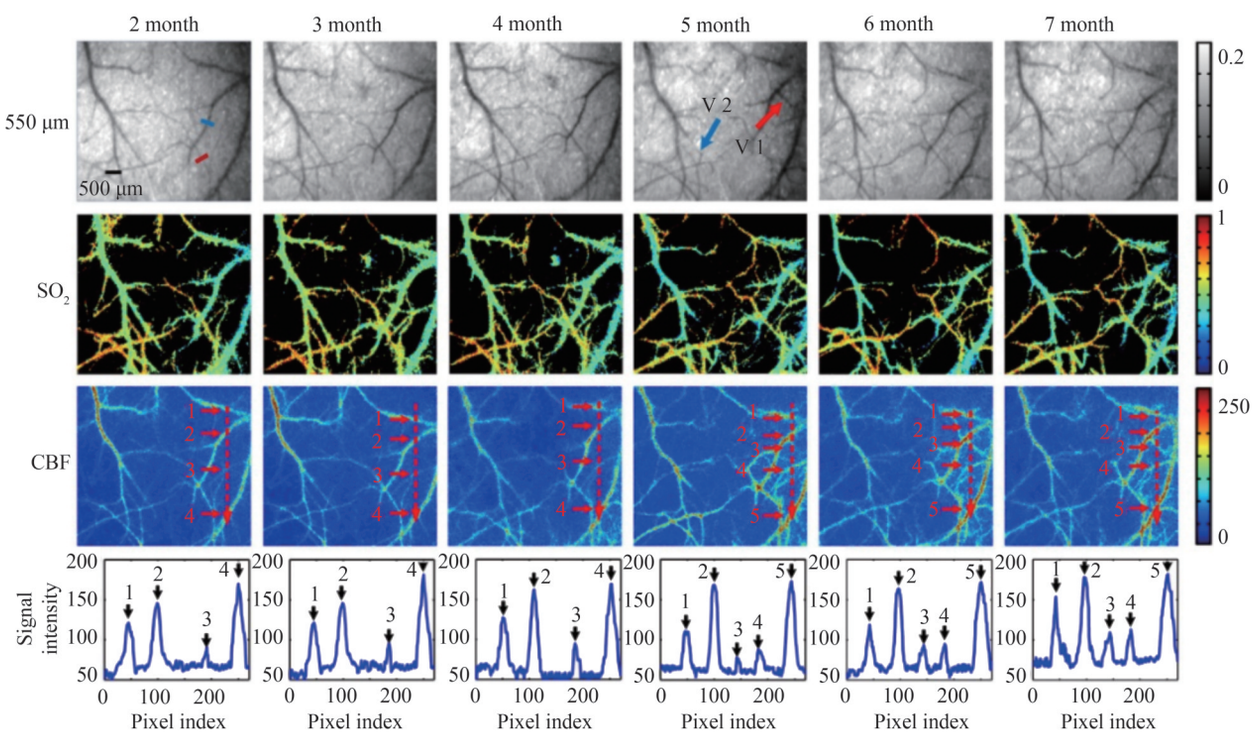

图3　基于USOCA的重复光透明成像用于皮层血流和血氧监测[54]

Fig.3　Repeatability of USOCA-based optical clearing imaging of cortical blood flow and blood oxygen [54]

糖尿病是一种慢性代谢性疾病，因此有监测糖尿病不同发展阶段体内脑血管功能障碍的变化具有与重要意义。FENG Wei等[61]透过基于USOCA建立的颅骨光透明窗，对一型糖尿病发展过程中，小鼠皮层血流和血氧对扩血管药物硝普化钠的响应变化进行了可视化研究。结果表明，对于健康小鼠，静脉注射硝普化钠后，皮层血流值会快速下降，然后快速上升并超过基线值，最终恢复至静息状态的数值；皮层血氧饱和度对硝普化钠的响应也与血流响应类似。但是，随着糖尿病病程的发展，皮层血流响应会显著下降，而血氧响应则会显著上升，这表示长期的高血糖环境使得皮层血管功能发生异常。

2.3　深皮层血管可视化

在体皮层成像深度可以从侧面反应光透明颅窗的透明度，因此研究人员经常会设计相关实验，探索发展的颅骨光透明方法对于深组织血管和神经细胞的成像能力。ZHANG Chao等[54]探究了USOCA的深组织成像能力，发现颅骨光透明之前，双光子荧光显微镜仅能获取深度在120 μm之内的大血管（直径67.5 μm）的结构信息，而颅骨透明后则可以对300 μm深的毛细血管（直径4.5 μm）进行观测。

CHEN Yage等[55]探究了SOCW与USOCA相结合获取深皮层血管信息的能力，他们对颅骨依次进行

胶原解离、脱脂、脱钙和和折射率匹配后，利用三光子荧光显微镜达到了850 μm的成像深度。

LI Dongyu等[51]探究了VNSOCA用于近红外二区激发的皮层深组织非线性成像的能力。利用1 560 nm激发的三倍频信号，可以获取650 μm的深层毛细血管信息，该深度是不进行颅骨光透明时的3倍，接近与开颅状态下的结果(800 μm)。图4展示了光透明颅窗用于三光子成像和三倍频成像的结果。

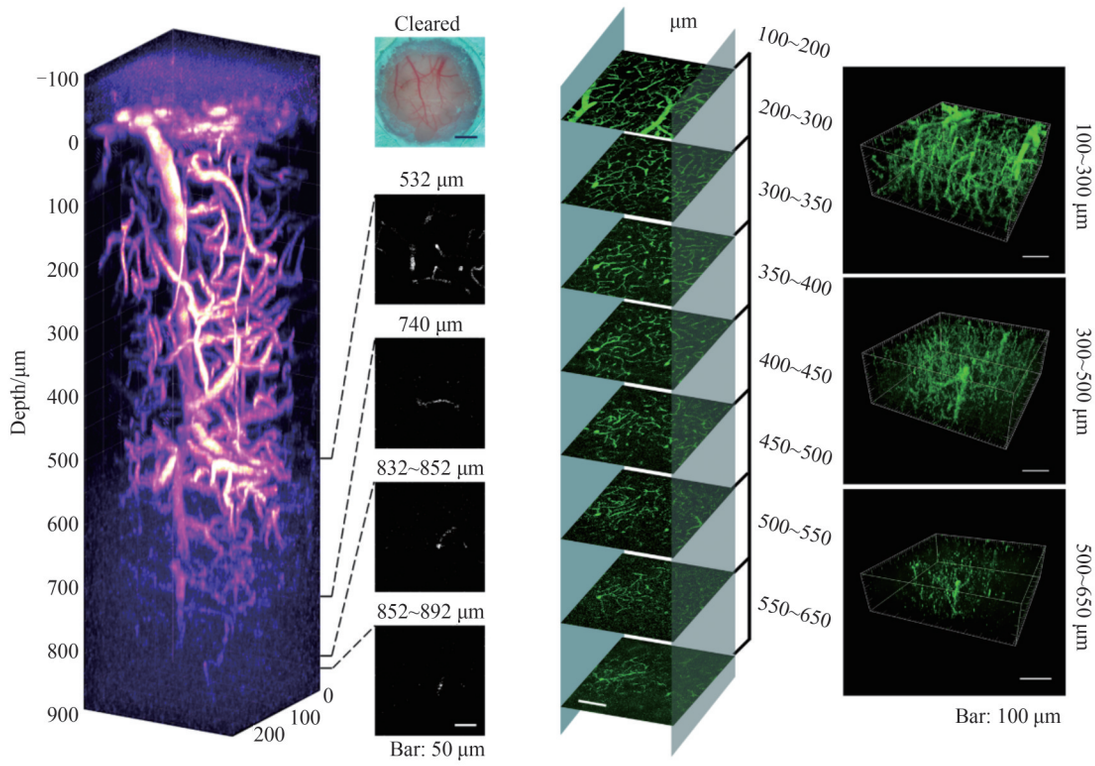

(a) Three-photon fluorescence imaging based on USOCA+SOCW　　(b) THG imaging based on VNSOCA

图4 光透明颅窗用于深皮层血管非线性成像[51,55]

Fig.4 Skull optical clearing window for nonlinear optical imaging of deep cortical vasculature [51,55]

3 活体颅骨光透明用于皮层光操控

现代光学技术不仅可以获得高分辨率的神经血管图像，而且可以对大脑皮层进行操控或建立特定的模型。基于颅骨光透明技术的窗口，也可替代开颅窗和磨薄窗，用于皮层光操控。比如，结合光透明颅窗和光动力效应，既可以打开血脑屏障，也可以建立靶向缺血性脑卒中模型；此外，透过光透明颅窗，将飞秒激光聚焦在血管上，可以实现对单根血管的烧蚀，从而建立局部靶向的出血性脑卒中模型。

3.1 光动力效应打开血脑屏障

血脑屏障在中枢神经系统中起着重要作用[79-80]。它能阻止血液中的有害物质进入脑实质，从而维持大脑的正常功能[81]，同样也会屏蔽许多神经药物[82]而影响治疗。为了特定的药物递送，需要暂时打开血脑屏障[83-90]，而利用光动力效应打开血脑屏障的方法得到了广泛关注[91-92]。

光动力效应是指光敏剂在特定波长的光的照射下会产生单线态氧、进而产生毒理性的化学反应的过程。显然，利用光动力效应产生的单线态氧能够影响血管内皮细胞功能，使得光照部位周围的血脑屏障被打开[92]。靶向打开血脑屏障，要求光能够在不被颅骨散射的情况下到达皮层的目标区域。即使是非靶向地利用光动力效应打开血脑屏障，如果不对颅骨进行开窗处理，就需要提高光功率，而这往往会造成严重的血管性水肿。

ZHANG Chao等[62]利用光透明颅窗，在不开颅的情况下实现了光动力效应打开血脑屏障。离体实验结果表明，光透明颅窗建立后，静脉注射光敏剂和荧光小分子伊文思蓝(961 Da)，激光照射皮层会引起血管伊文思蓝的外渗，而同等剂量下不对颅骨进行透明化处理并未在组织中观察到伊文思蓝。FENG Wei等[63]同

样在光透明颅窗下利用光动力效应打开血脑屏障，并在活体水平跟踪了伊文思蓝的渗漏过程。除了小分子，他们还证明光透明颅窗结合光动力效应也可以向脑实质中运送右旋糖酐（Rhodamine-dextran-70 kDa，图5）和脂质体（粒径100 nm）等大分子。

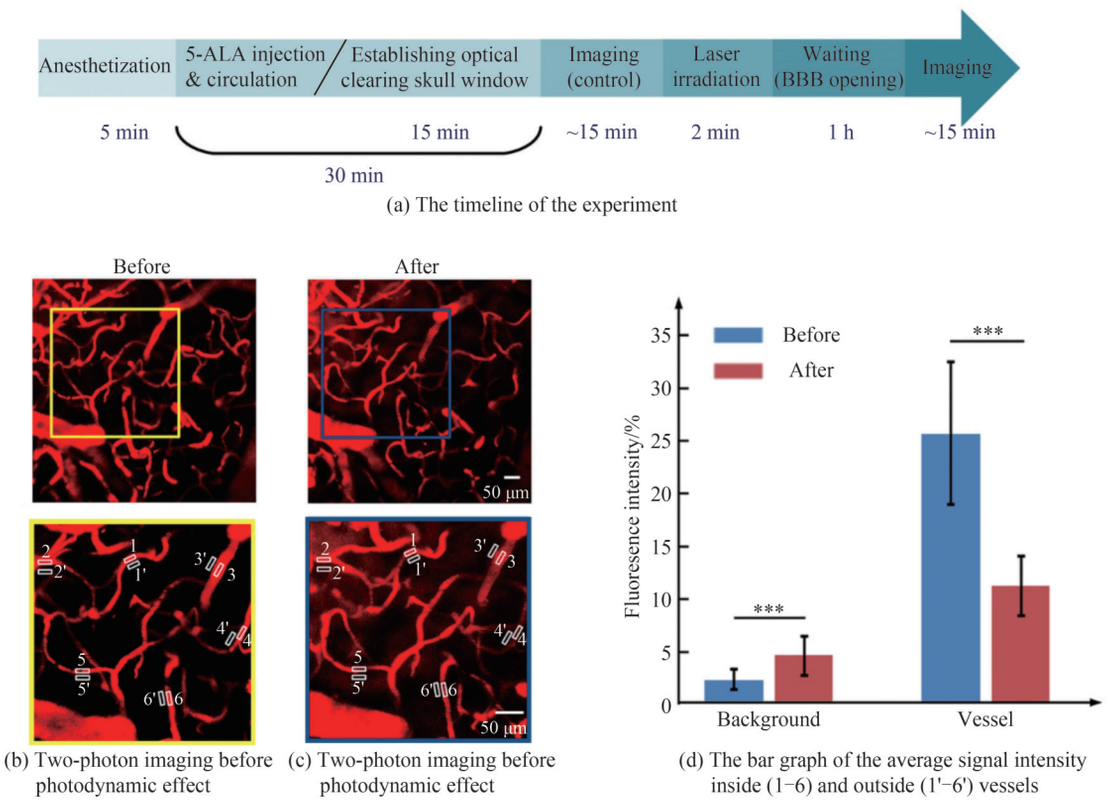

(a) The timeline of the experiment

(b) Two-photon imaging before photodynamic effect

(c) Two-photon imaging before photodynamic effect

(d) The bar graph of the average signal intensity inside (1-6) and outside (1'-6') vessels

图5　光透明颅窗结合光动力效应打开血脑屏障后利用双光子显微镜观察血管中Rhodamine-dextran的渗漏情况[62]

Fig.5　Skull optical clearing window combined with photodynamic effect for blood brain barrier opening and two-photon fluorescence observing of the leakage of Rhodamine-Dextran in blood vessels [62]

进一步地，ZHANG Chao等[93]研究了光动力效应不同年龄小鼠（2/4/6/8周龄）血脑屏障功能影响的差异性。结果表明，年轻小鼠的血脑屏障更易受光动力效应的调控，从而能允许大分子透过。

3.2　建立靶向脑卒中模型

少量的单线态氧可以影响血管内皮细胞功能，从而打开血脑屏障，而大剂量的单线态氧可以损伤内皮细胞，造成血小板聚集，形成血栓。因此，利用光动力效应可以建立缺血性脑卒中模型，也称为光栓模型，被广泛应用于对缺血性脑卒中的研究当中。传统的靶向光栓模型需要在开颅的情况下建立，但开颅引发的颅内压变化和炎症，使得大脑在卒中建立之前就处在非正常的环境当中，从而对观测结果产生影响。

HU Zhengwu等[64]将USOCA与光栓技术相结合，在非开颅的情况下，实现了对大脑皮层血管的靶向栓塞。改变激光照射位置和照射剂量，方便地对栓塞程度和栓塞区域进行调节。

在传统的光栓模型中，栓子的主要成分是血小板[94-95]，但是临床上栓子的主要成分包括血小板和纤维蛋白[96-97]，并且纤维蛋白才是大部分溶栓药物的有效靶点。因此，传统的光栓不适合用于对溶栓药物的研究。2020年，SUN Yuyo等[98]提出了一种改进的光栓模型，通过将凝血酶与光敏剂同时注射到小鼠的循环系统，激光照射后会在血管中形成同时包含血小板和纤维蛋白的栓子，更接近于临床的情况。

LI Dongyu等[65]将光透明颅窗与改进的光栓模型相结合，分别对大脑中动脉、大脑中动脉二级分支和大脑中动脉远端小血管建立了靶向缺血性脑卒中模型，用于研究临床药物尿激酶对不同尺寸血管的溶栓治疗效果。结果表明，对于小尺寸的远端小血管，尿激酶溶栓时间最短，但容易形成二次堵塞；对于大尺寸的大脑中动脉，尿激酶溶栓时间长，且溶栓不完全；对于大脑中动脉二级分支，尿激酶能比较好的实现血管再通，并且在一天后仍未出现二次堵塞现象（图6）。

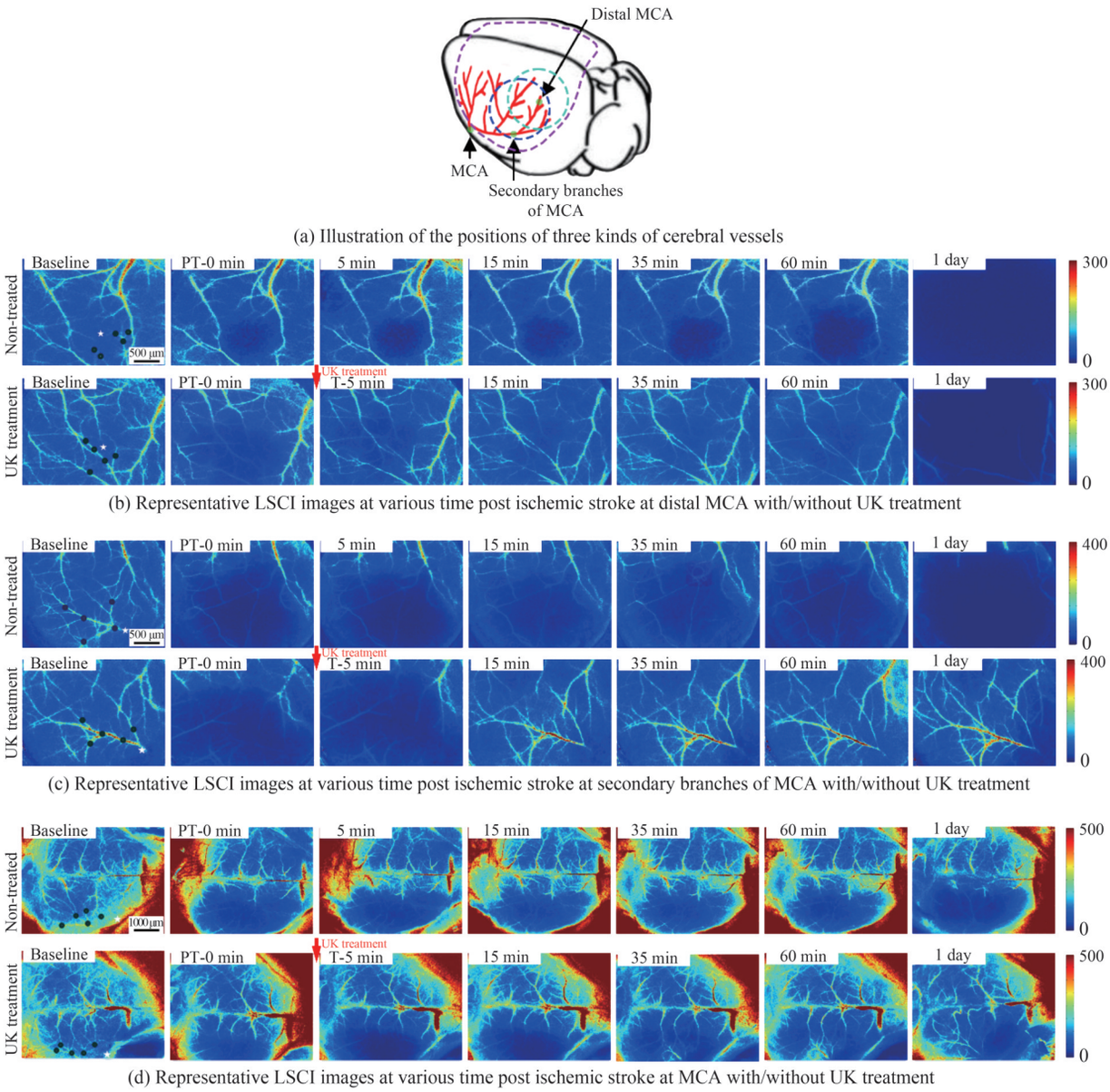

图 6 光透明颅窗用于建立靶向光栓模型及尿激酶对不同尺寸血管溶栓效果评估[65]

Fig.6 Skull optical clearing window for establishment of targeted photothrombosis and evaluation of thrombolytic effect of urokinase for vessels with different sizes [65]

激光损伤模型因其损伤范围和部位易于控制而被广泛应用[99-100]。LI Dongyu 等[51]透过光透明颅窗，将近红外Ⅱ区的飞秒激光聚焦，实施了对皮层血管的靶向烧蚀，成功地建立了单血管出血性脑卒中模型。实验表明，在直径较小和直径较大的血管上都可以建立该模型。并且，实验人员利用光透明颅窗和三倍频显微镜，能够观测到血管损伤出血、血液扩散到血管损伤位点凝血的全过程。

4 总结与展望

近年发展的颅骨光透明技术为活体皮层观测提供了一个无需开颅的光学窗口。十年来，随着技术的不断发展，至今已有多种光透明颅窗可供选择，它们各有特点。SOCW 的作用机理是，对幼年小鼠颅骨进行胶原解离，对成年小鼠颅骨进行脱钙，并用甘油进行折射率匹配。它能对皮层浅层区域实现突触分辨。但是，由于没有引入促渗剂，用于成年小鼠时需要预先将颅骨打磨至 100 μm 厚。USOCA 通过乙醇和尿素来解离胶原并促进渗透，并用十二烷基苯磺酸钠进行去脂。它不需要对颅骨进行打磨，可以适用于最老 8 月龄的小鼠，并能实现 5 个月的长期重复透明观测。将 SOCW 和 USOCA 结合，同时去除颅骨的羟基磷灰石、胶原蛋

白和脂质，可以进一步提高颅骨的透明度，从而实现三光子深皮层血管成像。VNSOCA将USOCA中的水替换为重水，大大提高了其对近红外Ⅱ区的透过率，同样能借助三倍频显微镜实现深皮层血管成像。近期，LI Dongyu等[101]在bioRxiv公开了一种长效光透明颅窗，能使得小鼠颅骨在数周之内保持透明，以供重复成像。同时，发表的新型光透明颅窗可以用于清醒动物神经元响应以及光遗传学研究，进一步拓展了光透明颅窗的适用范围。

随着新型光透明颅窗的出现，光声成像、激光散斑成像、高光谱成像和非线性显微成像等多种光学成像技术被应用于活体观察皮层神经元、小胶质细胞、血管结构和功能。借助光透明颅窗，可以动态观测神经突触可塑性、神经元自发发放或对刺激的响应、长时程监测血管的修剪与新生、表层与深层的血液流速变化等。光学相干层析成像技术是一种非标记的层析成像技术，可以在活体水平观测组织或血管的三维结构[102]，借助手术颅窗，该技术在脑科学研究中已得到广泛应用[103]。研究表明，活体皮肤光透明技术可以显著增强光学相干层析成像在皮肤中的成像质量，有助于获取皮肤深组织信息。因此，将光透明颅窗技术与光学相干层析成像技术相结合，有潜力在无需标记的情况下获取皮层深组织的血管结构与功能信息。不仅如此，颅骨光透明技术也为皮层靶向光操控提供了非侵入性的窗口。利用飞秒激光，可以实现神经血管的靶向损伤，结合光动力效应，可以实现血脑屏障的开放或建立光栓模型。

不同的脑科学研究对颅窗提出了不同的要求。比如，神经突触成像需要高分辨观测，许多疾病的研究需要长时程跟踪[66-67]，急性病理模型需要建窗口立即观测[104-106]，神经功能成像需要在清醒动物上开展[107-108]，跨脑区研究需要较大的观测视场[109]。开颅玻璃窗无法实现急性观测，磨薄颅骨窗无法实现大视场观测。而光透明颅窗发展至今，已同时具备了高分辨、大视场、长时程、适用于急性观测的优势，因而有望在某些传统颅窗无法胜任的场合（比如急性创伤性脑损伤[110-111]的跨脑区观测）提供重要的技术支撑，从而在未来的脑科学研究中大放异彩。

诚然，目前颅骨光透明技术依然有所限制。比如，目前尚未有适用于更大动物（比如大鼠、猕猴等）的活体颅骨光透明方法，这需要研究人员继续探索更高效的颅骨光透明方法。一方面，可以筛选折射率更高的试剂用于折射率匹配；另一方面，需要发展更有效的物理或化学促渗方法，帮助光透明试剂充分作用于更厚的颅骨。另外，相较于开颅玻璃窗和磨薄颅骨窗的平面结构，光透明颅窗维持了颅骨的曲面结构，虽然这使得大脑在被观测时更接近于生产生理状态，但是，曲面的颅窗给成像带来更多像差，并且会限制小景深成像系统的应用。在未来，可以通过自适应光学技术[112-113]，为基于颅骨光透明的成像进行波前矫正，同时期待大视场、高分辨且同时拥有大焦深的成像技术（比如光场显微镜[114]）与光透明颅窗的结合。

参考文献

[1] LAVISSE S, GOUTAL S, CWIMBERLEY, et al. Increased microglial activation in patients with Parkinson disease using [18F]-DPA714 TSPO PET imaging[J]. Parkinsonism & Related Disorders, 2021, 82: 29-36.

[2] JOVIN T G, NOGUEIRA R G, GLANSBERG M, et al. Thrombectomy for anterior circulation stroke beyond 6 h from time last known well (AURORA): a systematic review and individual patient data meta-analysis[J]. Lancet, 2022, 399 (10321): 249-258.

[3] VILLEMAGNE V L, BARKHOF F, GARIBOTTO V, et al. Molecular imaging approaches in dementia[J]. Radiology, 2021, 298 (3): 517-530.

[4] JONAS OGIEN A D, MAXINE C, JEAN-LUC P, et al. Line-field confocal optical coherence tomography for three-dimensional skin imaging[J]. Frontiers of Optoelectronics, 2020, 13 (4): 381-392.

[5] CHENG Zhongwen, MA Haigang, WANG Zhiyang, et al. *In vivo* volumetric monitoring of revascularization of traumatized skin using extended depth-of-field photoacoustic microscopy[J]. Frontiers of Optoelectronics, 2020, 13 (4): 307-317.

[6] WANG Xiaohui, LI Zhipeng, DING Yadan, et al. Enhanced photothermal-photodynamic therapy for glioma based on near-infrared dye functionalized Fe_3O_4 superparticles[J]. Chemical Engineering Journal, 2020, 381: 122693-122693.

[7] YAKOVLEV D V, FARRAKHOVA D S, SHIRYAEV A A, et al. New approaches to diagnostics and treatment of cholangiocellular cancer based on photonics methods[J]. Frontiers of Optoelectronics, 2020, 13 (4): 352-359.

[8] KAZACHKINA N, LYMAR J, SHCHESLAVSKIY V, et al. A pilot study of the dynamics of tissue oxygenation *in vivo* using time-resolved phosphorescence imaging[J]. Journal of Innovative Optical Health Sciences, 2021, 14 (5): 2142001.

[9] LEI Zhao, ZENG Yun, ZHANG Xiaofen, et al. Photoacoustic reporter genes for noninvasive molecular imaging and theranostics[J]. Journal of Innovative Optical Health Sciences, 2020, 13 (3): 2030005.

[10] YANG Wenzhao, CHEN S. Time-gated fluorescence imaging: advances in technology and biological applications[J]. Journal of Innovative Optical Health Sciences, 2020, 13(3): 12-31.
[11] HONG Guosong, ANTARIS A L, DAI Hongjie. Near-infrared fluorophores for biomedical imaging[J]. Nature Biomedical Engineering, 2017, 1(1): 0010.
[12] FAN Jianglan, RIVERA J A, SUN Wei, et al. High-speed volumetric two-photon fluorescence imaging of neurovascular dynamics[J]. Nature Communication, 2020, 11(1): 6020.
[13] KISLER K, LAZIC D, SWEENEY M D, et al. *In vivo* imaging and analysis of cerebrovascular hemodynamic responses and tissue oxygenation in the mouse brain[J]. Nature Protocols, 2018, 13(6): 1377-1402.
[14] LI Dongyu, XIA Qing, YU Tingting, et al. Transmissive-detected laser speckle contrast imaging for blood flow monitoring in thick tissue: from Monte Carlo simulation to experimental demonstration[J]. Light: Science & Applications, 2021, 10(1): 241.
[15] KISLER K, NIKOLAKOPOULOU A M, ZLOKOVIC B V. Microglia have a grip on brain microvasculature[J]. Nature Communications, 2021, 12(1): 5290.
[16] LEE S, NAMGOONG J M, KIM Y, et al. Multimodal imaging of laser speckle contrast imaging combined with mosaic filter-based hyperspectral imaging for precise surgical guidance[J]. IEEE Transactions on Biomedical Engineering, 2022, 69(1): 443-452.
[17] MARTINEZ-VEGA B, LEON R, FABELO H, et al. Oxygen saturation measurement using hyperspectral imaging targeting real-time monitoring[C]. 24th Euromicro Conference on Digital System Design (DSD), 2021:480-487.
[18] RAVI D, FABELO H, CALLIC G M, et al. Manifold embedding and semantic segmentation for intraoperative guidance with hyperspectral brain imaging[J]. IEEE Transactions on Medical Imaging, 2017, 36(9): 1845-1857.
[19] HUSSAIN A, PETERSEN W, STALIEY J, et al. Quantitative blood oxygen saturation imaging using combined photoacoustics and acousto-optics[J]. Optics Letters, 2016, 41(8):1720-1723.
[20] CHEN C, WANG Ruikang. Optical coherence tomography based angiography[J]. Biomedical Optics Express, 2017, 8(2): 1056-1082.
[21] MONTEIRO-HENRIQUES I, ROCHA-SOUSA A, BARBOSA-BREDA J. Optical coherence tomography angiography changes in cardiovascular systemic diseases and risk factors: a review[J]. Acta Ophthalmologica, 2022, 100(1): e1-e15.
[22] SUN Bin, WANG Mengran, HOERDER S A, et al. Intravital imaging of the murine subventricular zone with three photon microscopy[J]. Cerebral Cortex, 2022, 32(14): 3057-3067.
[23] WANG Tianyu, XU C. Three-photon neuronal imaging in deep mouse brain[J]. Optica, 2020, 7(8): 947-960.
[24] WANG Tianyu, OUZOUNOV D G, WU Chunyan, et al. Three-photon imaging of mouse brain structure and function through the intact skull[J]. Nature Methods, 2018, 15(10): 789-792.
[25] WEISENBURGER S, TEJERA F, DEMAS J, et al. Volumetric Ca^{2+} imaging in the mouse brain using hybrid multiplexed sculpted light microscopy[J]. Cell, 2019, 177(4): 1050-1066.
[26] CHEN Wei, NATAN R G, YANG Yuhan, et al. *In vivo* volumetric imaging of calcium and glutamate activity at synapses with high spatiotemporal resolution[J]. Nature Communications, 2021, 12(1): 6630.
[27] LU Fei, CAO Jiating, SU Qinglun, et al. Recent advances in fluorescence imaging of traumatic brain injury in animal models[J]. Frontiers in Molecular Biosciences, 2021, 8: 660993.
[28] ZHANG Haochen, YU Dongqin, LIU Shuting, et al. NIR-Ⅱ Hydrogen-Bonded Organic Frameworks (HOFs) used for target-specific amyloid-β photooxygenation in an alzheimer's disease model[J]. Angewandte Chemie International Edition, 2022, 61(2): e202109068.
[29] KNEIPP M, TURNER J, ESTRADA H, et al. Effects of the murine skull in optoacoustic brain microscopy[J]. Journal of Biophotonics, 2016, 9(1-2): 117-123.
[30] FAN Xiaofeng, ZHENG Weitao, SINGH D. Light scattering and surface plasmons on small spherical particles[J]. Light-Science & Applications, 2014, 3: e179.
[31] HOLTMAAT A, BONHOEFFER T, CHOW D K, et al. Long-term, high-resolution imaging in the mouse neocortex through a chronic cranial window[J]. Nature Protocols, 2009, 4(8): 1128-1144.
[32] YANG Guang, PAN Feng, PARKHURST C N, et al. Thinned-skull cranial window technique for long-term imaging of the cortex in live mice[J]. Nature Protocols, 2010, 5(2): 201-208.
[33] YANG Shanshan, LIU Kezhou, DING Huijie, et al. Longitudinal *in vivo* intrinsic optical imaging of cortical blood perfusion and tissue damage in focal photothrombosis stroke model[J]. Journal of Cerebral Blood Flow and Metabolism, 2019, 39(7): 1381-1393.
[34] DORAND R D, BARKAUSKAS D S, EVANS T A, et al. Comparison of intravital thinned skull and cranial window approaches to study CNS immunobiology in the mouse cortex[J]. Intravital, 2014, 3(2): e21978.
[35] DREW P J, SHIH A Y, DRISCOLL J D, et al. Chronic optical access through a polished and reinforced thinned skull[J].

Nature Methods, 2010, 7(12): 981-U960.
[36] MANGLANI M, MCGAVERN D B. Intravital imaging of neuroimmune interactions through a thinned skull[J]. Current Protocols in Immunology, 2018, 120(1): 24.2.1-24.2.12.
[37] COELHO-SANTOS V, BERTHIAUME A A, ORNELAS S, et al. Imaging the construction of capillary networks in the neonatal mouse brain[J]. Proceedings of the National Academy of Sciences of the United States of America, 2021, 118(26): e2100866118.
[38] ZHU Jingtan, LIU Xiaomei, DENG Yating, et al. Tissue optical clearing for 3D visualization of vascular networks: a review[J]. Vascular Pharmacology, 2021, 141: 106905.
[39] YU Tingting, ZHU Jingtan, LI Dongyu, et al. Physical and chemical mechanisms of tissue optical clearing[J]. Iscience, 2021, 24(3):102178.
[40] WAN Peng, ZHU Jingtan, XU Jianyi, et al. Evaluation of seven optical clearing methods in mouse brain [J]. Neurophotonics, 2018, 5(3):035007.
[41] YU Tingting, ZHU Jingtan, LI Yusha, et al. RTF: a rapid and versatile tissue optical clearing method[J]. Scientific Reports, 2018, 8: 1964.
[42] WAN Peng, ZHU Jingtan, YU Tingting, et al. Comparison of seven optical clearing methods for mouse brain[J]. Neural Imaging and Sensing, 2018, 2018: 10481.
[43] YU Tingting, ZHU Jingtan, LI Yusha, et al. ReagentTF: a rapid and versatile optical clearing method for biological imaging[J]. Neural Imaging and Sensing, 2017, 10051.
[44] YU Tingting, QI Yisong, WANG Jianru, et al. Rapid and prodium iodide-compatible optical clearing method for brain tissue based on sugar/sugar-alcohol[J]. Journal of Biomedical Optics, 2016, 21(8):81203.
[45] GENIN V D, GENINA E A, TUCHIN V V, et al. Glycerol effects on optical, weight and geometrical properties of skin tissue[J]. Journal of Innovative Optical Health Sciences, 2021, 14(5): 2142006.
[46] GENINA E A, SURKOV Y I, SEREBRYAKOVA I A, et al. Rapid ultrasound optical clearing of human light and dark skin[J]. IEEE transactions on medical imaging, 2020, 39(10): 3198-3206.
[47] ENFIELD J, MCGRATH J, DALY S M, et al. Enhanced *in vivo* visualization of the microcirculation by topical application of fructose solution confirmed with correlation mapping optical coherence tomography[J]. Journal of Biomedical Optics, 2016, 21(8): 081212.
[48] WANG Jing, ZHANG Yang, XU Tonghui, et al. An innovative transparent cranial window based on skull optical clearing [J]. Laser Physics Letters, 2012, 9(6): 469-473.
[49] GENINA E A, BASHKATOV A N, TUCHIN V V. Optical clearing of cranial bone [J]. Advances in Optical Technologies, 2008, 2008: 267867.
[50] CHEN Yage, LIU Shaojun, LIU Hongji, et al. Coherent Raman scattering unravelling mechanisms underlying skull optical clearing for through-skull brain imaging[J]. Analytical Chemistry, 2019, 91(15): 9371-9375.
[51] LI Dongyu, ZHENG Zheng, YU Tingting, et al. Visible-near infrared-Ⅱ skull optical clearing window for *in vivo* cortical vasculature imaging and targeted manipulation[J]. Journal of Biophotonics, 2020, 13(10): e202000142.
[52] YANG Xiaoquan, ZHANG Yang, ZHAO Kai, et al. Skull optical clearing solution for enhancing ultrasonic and photoacoustic imaging[J]. IEEE Transactions on Medical Imaging, 2016, 35(8): 1903-1906.
[53] ZHAO Yanjie, YU Tingting, ZHANG Chao, et al. Skull optical clearing window for *in vivo* imaging of the mouse cortex at synaptic resolution[J]. Light-Science & Applications, 2018, 7(2): 17153.
[54] ZHANG Chao, FENG Wwei, ZHAO Yanjie, et al. A large, switchable optical clearing skull window for cerebrovascular imaging[J]. Theranostics, 2018, 8(10): 2696-2708.
[55] CHEN Yage, LIU Shaojun, LIU Hongjie, et al. Coherent Raman scattering unravelling mechanisms underlying skull optical clearing for through-skull brain imaging[J]. Analytical Chemistry, 2019, 91(15): 9371-9375.
[56] WELSHER K, SHERLOCK S P, DAI Hongjie. Deep-tissue anatomical imaging of mice using carbon nanotube fluorophores in the second near-infrared window[J]. Proceedings of the National Academy of Sciences of the United States of America, 2011, 108(22): 8943-8948.
[57] WAN Hao, YUE Jingying, ZHU Shoujun, et al. A bright organic NIR-Ⅱ nanofluorophore for three-dimensional imaging into biological tissues[J]. Nature Communications, 2018, 9: 1171.
[58] ZHANG Mingxi, YUE Jingying, CUI Ran, et al. Bright quantum dots emitting at similar to 1,600 nm in the NIR-Ⅱb window for deep tissue fluorescence imaging[J]. Proceedings of the National Academy of Sciences of the United States of America, 2018, 115(26): 6590-6595.
[59] YU Wenbin, GUO Bin, ZHANG Hequn, et al. NIR-Ⅱ fluorescence *in vivo* confocal microscopy with aggregation-induced emission dots[J]. Science Bulletin, 2019, 64(6): 410-416.
[60] QI Ji, SUN Chaowei, ZEBIBULA A, et al. Real-time and high-resolution bioimaging with bright aggregation-induced emission dots in short-wave infrared region[J]. Advanced Materials, 2018, 30(12): 1706856.

[61] FENG Wei, LIU Shaojun, ZHANG Chao, et al. Comparison of cerebral and cutaneous microvascular dysfunction with the development of type 1 diabetes [J]. Theranostics, 2019, 9 (20): 5854-5868.
[62] ZHANG Chao, FENG Wei, VODOVOZOVA E, et al. Photodynamic opening of the blood-brain barrier to high weight molecules and liposomes through an optical clearing skull window[J]. Biomedical Optics Express, 2018, 9 (10): 4850-4862.
[63] FENG Wei, ZHANG Chao, YU Tingting, et al. *In vivo* monitoring blood-brain barrier permeability using spectral imaging through optical clearing skull window[J]. Journal of Biophotonics, 2019, 12 (4): e201800330.
[64] HU Zhengwu, LI Dongyu, ZHONG Xiang, et al. *In vivo* tissue optical clearing assisted through-skull targeted photothrombotic ischemic stroke model in mice[J]. Journal of Biomedical Optics, 2022, 27 (6): 065001.
[65] LI Dongyu, DENG Lu, HU Zhengwu, et al. Optical clearing imaging assisted evaluation of urokinase thrombolytic therapy on cerebral vessels with different sizes[J]. Biomedical Optics Express, 2022, 13 (6): 3243-3258.
[66] GUO Lili, XIONG Huan, KIM J I, et al. Dynamic rewiring of neural circuits in the motor cortex in mouse models of Parkinson's disease[J]. Nat Neurosci, 2015, 18 (9): 1299-1309.
[67] DROMARD Y, ARANGO-LIEVANO M, FONTANAUD P, et al. Dual imaging of dendritic spines and mitochondria *in vivo* reveals hotspots of plasticity and metabolic adaptation to stress[J]. Neurobiology of Stress, 2021, 15: 100402.
[68] XU Tonghui, YU Xinzhu, PERLIK A J, et al. Rapid formation and selective stabilization of synapses for enduring motor memories[J]. Nature, 2009, 462 (7275): 915-919.
[69] YU Xinzhu, WANG G, GILMORE A, et al. Accelerated experience-dependent pruning of cortical synapses in ephrin-A2 knockout mice[J]. Neuron, 2013, 80 (1): 64-71.
[70] XU Tonghui, WANG Shaofang, LALCHANDANI R R, et al. Motor learning in animal models of Parkinson's disease: Aberrant synaptic plasticity in the motor cortex[J]. Mov Disord, 2017, 32 (4): 487-497.
[71] DERBIE A Y. Neural mechanisms of spatial coding : a multimodal imaging study[D]. The Hong Kong Polytechnic University, 2021.
[72] DENG W, TSUBOTA K I. Numerical simulation of the vascular structure dependence of blood flow in the kidney[J]. Medical Engineering & Physics, 2022, 104: 103809.
[73] KIM Y, LEE Y B, BAE S K, et al. Development of a photochemical thrombosis investigation system to obtain a rabbit ischemic stroke model[J]. Scientific Reports, 2021, 11 (1): 5787.
[74] DRAIJER M, HONDEBRINK E, VAN LEEUWEN T, et al. Review of laser speckle contrast techniques for visualizing tissue perfusion[J]. Lasers in Medical Science, 2009, 24 (4): 639-651.
[75] BOAS D A, DUNN A K. Laser speckle contrast imaging in biomedical optics[J]. Journal of Biomedical Optics, 2010, 15 (1): 011109.
[76] GUILBERT J, DESJARDINS M. Movement correction method for laser speckle contrast imaging of cerebral blood flow in cranial windows in rodents[J]. Journal of Biophotonics, 2022, 15 (1): e202100218.
[77] KHAODHIAR L, DINH T, SCHOMACKER K T, et al. The use of medical hyperspectral technology to evaluate microcirculatory changes in diabetic foot ulcers and to predict clinical outcomes[J]. Diabetes Care, 2007, 30 (4): 903-910.
[78] YUDOVSKY D, NOUVONG A, SCHOMACKER K, et al. Monitoring temporal development and healing of diabetic foot ulceration using hyperspectral imaging[J]. Journal of Biophotonics, 2011, 4 (7-8): 565-576.
[79] RISAU W, WOLBURG H. Development of the blood-brain-barrier [J]. Trends in Neurosciences, 1990, 13 (5): 174-178.
[80] ABBOTT N J, ROMERO I A. Transporting therapeutics across the blood-brain barrier[J]. Molecular Medicine Today, 1996, 2 (3): 106-113.
[81] EL-BACHA R S, MINN A. Drug metabolizing enzymes in cerebrovascular endothelial cells afford a metabolic protection to the brain[J]. Molecular and Cellular Biology, 1999, 45 (1): 15-23.
[82] PARDRIDGE W M. Molecular Trojan horses for blood-brain barrier drug delivery[J]. Current Opinion in Pharmacology, 2006, 6 (5): 494-500.
[83] PATEL M M, PATEL B M. Crossing the blood-brain barrier: recent advances in drug delivery to the brain[J]. Cns Drugs, 2017, 31 (2): 109-133.
[84] MITRAGOTRI S. Devices for overcoming biological barriers: The use of physical forces to disrupt the barriers[J]. Advanced Drug Delivery Reviews, 2013, 65 (1): 100-103.
[85] HERSH D S, WADAJKAR A S, ROBERTS N B, et al. Evolving drug delivery strategies to overcome the blood brain barrier[J]. Current Pharmaceutical Design, 2016, 22 (9): 1177-1193.
[86] KIVINIEMI V, KORHONEN V, KORTELAINEN J, et al. Real-time monitoring of human blood-brain barrier disruption[J]. Plos One, 2017, 12 (3): e0174072.
[87] POON C, MCMAHON D, HYNYNEN K. Noninvasive and targeted delivery of therapeutics to the brain using focused ultrasound[J]. Neuropharmacology, 2017, 120: 20-37.
[88] FISHMAN P S, FRENKEL V. Focused ultrasound: an emerging therapeutic modality for neurologic disease [J].

Neurotherapeutics, 2017, 14(2): 393-404.
[89] DHURIA S V, HANSON L R, FREY W H. Intranasal delivery to the central nervous system: mechanisms and experimental considerations[J]. Journal of Pharmaceutical Sciences, 2010, 99(4): 1654-1673.
[90] KARAISKOS I, GALANI L, BAZIAKA F, et al. Intraventricular and intrathecal colistin as the last therapeutic resort for the treatment of multidrug-resistant and extensively drug-resistant Acinetobacter baumannii ventriculitis and meningitis: a literature review[J]. International Journal of Antimicrobial Agents, 2013, 41(6): 499-508.
[91] HIRSCHBERG H, UZAL F A, CHIGHVINADZE D, et al. Disruption of the blood-brain barrier following ALA-mediated photodynamic therapy[J]. Lasers Surg Med, 2008, 40(8): 535-542.
[92] MADSEN S J, HIRSCHBERG H. Site-specific opening of the blood-brain barrier[J]. Journal of Biophotonics, 2010, 3(5-6): 356-367.
[93] ZHANG Chao, FENG Wei, LI Yusha, et al. Age differences in photodynamic therapy-mediated opening of the blood-brain barrier through the optical clearing skull window in mice[J]. Lasers in Surgery and Medicine, 2019, 51(7): 625-633.
[94] BRANT D. WATSON W D D, BUSTO R, et al. Induction of reproducible brain infarction by photochemically initiated thrombosis[J]. Annals of Neurology, 1985, 17: 497-504.
[95] WATSON B D, PRADO R, VELOSO A, et al. Cerebral blood flow restoration and reperfusion injury after ultraviolet laser-facilitated middle cerebral artery recanalization in rat thrombotic stroke[J]. Stroke, 2002, 33(2): 428-434.
[96] BACIGALUPPI M, SEMERANO A, GULLOTTA G S, et al. Insights from thrombi retrieved in stroke due to large vessel occlusion[J]. Journal of Cerebral Blood Flow and Metabolism, 2019, 39(8): 1433-1451.
[97] MARDER V J, CHUTE D J, STARKMAN S, et al. Analysis of thrombi retrieved from cerebral arteries of patients with acute ischemic stroke[J]. Stroke, 2006, 37(8): 2086-2093.
[98] SUN Y, KUO Yimin, CHEN Hongru, et al. A murine photothrombotic stroke model with an increased fibrin content and improved responses to tPA-lytic treatment[J]. Blood Advances, 2020, 4(7): 1222-1231.
[99] DAVALOS D, GRUTZENDLER J, YANG G, et al. ATP mediates rapid microglial response to local brain injury *in vivo*[J]. Nature Neuroscience, 2005, 8(6): 752-758.
[100] NIMMERJAHN A, KIRCHHOFF F, HELMCHEN F. Resting microglial cells are highly dynamic surveillants of brain parenchyma *in vivo*[J]. Science, 2005, 308(5726): 1314-1318.
[101] LI Dongyu, HU Zhengwu, ZHANG Hequn, et al. Solid optical clearing agents based through-Intact-Skull (TIS) window technique for long-term observation of cortical structure and function in mice[J]. bioRxiv, 2021, doi:10.1101/2021.10.02.462855.
[102] QIU Jianrong, HAN Tao, LIU Zhiyu, et al. Uniform focusing with an extended depth range and increased working distance for optical coherence tomography by an ultrathin monolith fiber probe[J]. Optics Letters, 2020, 45(4): 976-979.
[103] YU Yao, MENG Ziyue, LI Ang, et al. Monitoring of edema progression in permanent and transient MCAO model using SS-OCT[J]. Journal of Innovative Optical Health Sciences, 2021, 14(1): 2140006.
[104] HAN Xinjia, CHAI Z, PING Xingjie, et al. *In vivo* two-photon imaging reveals acute cerebral vascular spasm and microthrombosis after mild traumatic brain injury in mice[J]. Frontiers in Neuroscience, 2020, 14: 210.
[105] REN Huixia, YANG Zheng, LUO Chuanming, et al. Enriched endogenous Omega-3 fatty acids in mice ameliorate parenchymal cell death after traumatic brain injury[J]. Molecular Neurobiology, 2017, 54(5): 3317-3326.
[106] ROTH T L, NAYAK D, ATANASIJEVIC T, et al. Transcranial amelioration of inflammation and cell death after brain injury[J]. Nature, 2014, 505(7482): 223.
[107] ZHANG Jinfan, LIU Bian, HONG I, et al. An ultrasensitive biosensor for high-resolution kinase activity imaging in awake mice[J]. Nature Chemical Biology, 2021, 17(1): 39-46.
[108] ZONG Weijian, WU Runlong, LI Mingli, et al. Fast high-resolution miniature two-photon microscopy for brain imaging in freely behaving mice[J]. Nature Methods, 2017, 14(7): 713-719.
[109] FAN Jingtao, SUO Jinli, WU Jiamin, et al. Video-rate imaging of biological dynamics at centimetre scale and micrometre resolution[J]. Nature Photonics, 2019, 13(11): 809-816.
[110] SMITH L G F, MILLIRON E, HO M L, et al. Advanced neuroimaging in traumatic brain injury: an overview[J]. Neurosurgical Focus, 2019, 47(6): E17.
[111] AZIM A, JOSEPH B. Surgical critical care therapy: a clinically oriented practical approach[M]. Springer International Publishing, 2018.
[112] QIN Zhongya, HE Sicong, YANG Chao, et al. Adaptive optics two-photon microscopy enables near-diffraction-limited and functional retinal imaging *in vivo*[J]. Light: Science & Applications, 2020, 9(1): 1-11.
[113] STREICH L, BOFFI J C, WANG Ling, et al. High-resolution structural and functional deep brain imaging using adaptive optics three-photon microscopy[J]. Nature Methods, 2021, 18(10): 1253-1258.
[114] WANG Kai. Deep-learning-enhanced light-field microscopy[J]. Nature Methods, 2021, 18(5): 459-460.

In vivo Skull Optical Clearing Technique and its Applications (Invited)

LI Dongyu[1,2,3], YU Tingting[1,2,3], ZHU Jingtan[1,2,3], ZHU Dan[1,2,3]

(1 *Britton Chance Center for Biomedical Photonics & MoE Key Laboratory for Biomedical Photonics, Wuhan National Laboratory for Optoelectronics, Huazhong University of Science and Technology, Wuhan* 430074, *China*)

(2 *Advanced Biomedical Imaging Facility, Huazhong University of Science and Technology, Wuhan* 430074, *China*)

(3 *Optics Valley Laboratory, Wuhan* 430074, *China*)

Abstract: *In vivo* observation of cortical structure and activity is of great significance for understanding the brain functions in the normal state and neurovascular dysfunction associated with various brain diseases. Modern optical imaging techniques has attracted many attentions in the field of neuroscience because it provides an important tool to visualize brain *in vivo* with high resolution. However, the strong scattering of the turbid skull limits light penetration, causing a serious degradation of imaging depth and imaging quality. In order to overcome such an obstacle, various skull windows have been established to access. The surgery-based skull windows mainly include open-skull window and thinned-skull window which have been widely used for cortical optical imaging. The former allows for large-scale imaging and long-term observation. The latter requires to thin the skull to about 25 μm that spine-resolution cortical imaging can be performed. However, each of the two skull windows has its own limitations. The open-skull window would cause inflammation therefore is not suitable for immediate observation, and the thinned-skull window is not capable of large-scale or long-term observation. During the past 10 years, some novel skull window techniques have been developed based on tissue optical clearing technique. Unlike physically remove or thin out the skull, the establishment of the "skull optical clearing window" is realized by using chemical agents to make the skull transparent, therefore no craniotomy is required. Considering the main the components of skull are calcium hydroxyapatite (16%), collagen (16%), lipids (54%), and water (14%), and the refractive index of the calcium hydroxyapatite, collagen and lipids are much higher than water, leading to server scattering, the skull optical clearing technique aims to remove those scattering particles and match the refractive index.

WANG Jing et al. demonstrated a skull optical clearing window for the first time in 2012. They used a mixture of laurinol, weak alkaline substances, Ethylene Diamine Tetraacetic Acid, dimethyl sulfoxide, sorbitol, alcohol, and glucose to decrease the scattering of skull. Through the established craniotomy-free skull window, they obtained cortical blood flow distribution with laser spackle contrast imaging. The preliminary work attracted numerous attentions in the field of neural science. Later in 2018, ZHAO Yanjie et al. improved the technique. They used collagenase, Ethylene Diamine Tetraacetic Acid disodium and glycerol to make the skull transparent to monitor the plasticity of dendritic protrusions of juvenile mice during 1 hour with two-photon microscopy. ZHANG Chao et al. developed a switchable skull optical clearing technique for long-term monitoring. The main components of the new skull optical clearing agent were urea, ethanol, and sodium dodecylbenzenesulfonate. These agents could make skulls transparent in mice aged from 2 months to 8 months. Additionally, the authors performed skull optical clearing imaging of cortical vasculature once a month to achieve observations lasting months. In 2019, CHEN Yage et al. combined the above two skull optical clearing agents for higher skull transparency. The authors firstly used ethanol solution of urea to depolymerize the proteins in the skull, followed by the using of sodium dodecylbenzenesulfonate to dissolve the lipids, then used Ethylene Diamine Tetraacetic Acid to disintegrate the hydroxyapatite, and finally treated the skull with glycerol for refractive index matching. After the optical clearing process, they used three-photon fluorescence microscopy to achieve 850-μm imaging depth of cortical blood vessels. However, the previous skull optical clearing agents were not optimized for the NIR-Ⅱ region due to the strong absorption of the main component, water. To establish a skull optical clearing window compatible to with NIR-Ⅱ light, LI Dongyu et al. replaced water into deuteroxide as the solvent, remarkably increasing the transmittance of the optical clearing agents to NIR-Ⅱ light. Combined with NIR-Ⅱ excited third harmonic generation imaging, the imaging depth was 3 times higher than that without optical clearing, and was even close to that without skull. The above skull optical clearing agents are liquid-based, which means they are not suitable for long-lasting continuous observation

or for awake animals.

Except for optical imaging, the skull optical clearing windows have also been used for light-induced manipulation in brain cortex. Through the established optical clearing window, laser could be easily focused on tiny structures, such as blood capillary and neuron dendrites, to achieve targeted ablation. In addition, skull optical clearing window could be combined with photodynamic effect to realize blood-brain barrier opening or targeted photothrombosis.

In summary, the novel *in vivo* skull optical clearing technique provides an optical window for cortical observation without craniotomy. Over the past decades, with the development of technique, there are a variety of skull optical clearing windows available, each with its own characteristics. Through the skull optical clearing window, various modern optical imaging techniques have been used to noninvasively monitor neurovascular information. Up to now, the skull optical clearing window holds the advantages of high resolution, large scale, long-term observation, and is compatible with immediate observation, therefore has great potential in the research of brain science and related diseases.

Key words: *in vivo* skull optical clearing; Optical imaging; Optical manipulation; Neurovascular imaging; Photodynamic effect

OCIS Codes: 110.0113; 110.0180; 160.1435

Foundation item: National Natural Science Foundation of China (Nos. 61860206009, 81870934, 82001877), Innovation Fund of WNLO, Innovation Project of Optics Valley Laboratory (No. OVL2021BG011)